Study on Flow Behavior in Terminal Bronchus of Human Lung for Porous Medium

Sadiya Akhter[a*] and M. U. Ahmmed[b]

aDepartment of Quantitative Sciences, International University of Business Agriculture and Technology, Dhaka-1230, Bangladesh
bDepartment of Mathematics, Jahangirnagar University, Dhaka-1342, Bangladesh

ABSTRACT

Flow simulation along human lung channel is one of the interests of investigation in fluid dynamics. We have studied flow phenomena of 11th generation of human lung as porous medium. The governing equations of porous medium have been solved numerically using finite difference scheme. The effect of different flow parameters are illustrated graphically. It is observed that the flow rate increases for increasing the value of pressure gradient, the porosity effect, effective viscosity and the dimensionless parameter σ. The numerical experiment for non-porous medium is also studied. It is found that the flow rate increases in porous medium compared with non-porous medium.

1. Introduction

Numerical experiment is very interesting to know the flow behavior in human lung channel where in vivo knowledge it is very difficult. Flow phenomena in human lung is practically important because it has effects on respiratory gas exchange, particle assertion and oxygen diffusion [1]. The bifurcating airways are networking system for each generations whose length and diameter are very small. The respiratory tract does not take part in gas exchange without leading the air to the respiratory zone [2]. In 17th generation of lung model gas diffuses from higher concentration to lower concentration through thin membranes which is known as alveoli [3]. The effective viscosity of some very known fluids such as air, water, oils, oxygen and nitrogen has been investigated through porous medium [4]. Viscosity of the fluid is increased or decreased according to the base fluid viscosity.

---

*Corresponding Author. *Email Address:*sadiyarahmansm@gmail.com

Here it is observed that the effective viscosity is increased in porous medium for Newtonian fluid. In aerodynamics the flow simulation along porous medium is very important because of the fluid nature. Some practical examples of flow through porous medium are as seepage of ground water, the flow of fluids in porous duct , flow phenomena in human lung and the blood flow through vein. Researchers have find interest to investigate the flow behavior of the fluid through porous medium in different symmetry. The flow behavior of Non-Newtonian fluids in a duct of porous medium has been investigated [5]. Here the flow rate decreases for the effect of couple stress parameter and porosity parameter and the flow rate increases for the effect of Jeffrey parameter and pressure gradient. The interconnection of bio fluid flow and pulsate magneto fluid flow through porous medium is studied theoretically [6]. The example deals with a viscous incompressible fluid and transverse magnetic field with infinite parallel walls through porous medium. The effect of heat exchange and force field of fluid in pipe with porous space has been studied [7]. Here series solutions for non linear partial differential equations are first developed and then convergent to the obtained series solutions which has been discussed explicitly. The analytical solution of magneto fluid flow through porous medium between permeable surfaces is derived [8]. On that paper the velocity and volume flow rate are graphically presented for different parametric effects illustrating their phenomenal nature. The axial flow behavior is presented in a square duct with the effect of heat transfer using finite element method [9]. On that work the axisymmetric flow along the square duct has been represented with the effect of heat transfer in three dimensional plot. The flow phenomena for Newtonian fluid in a duct model has been shown with temperature effect and velocity distributions [10]. Here the laminar flow is developed to be parabolic with the effect of heat transfer that is indistinguish with thin plate theory. The laminar flow is graphically represented with the effect of heat transfer along a square duct for Herschel Bulkley fluid [11]. On that work the non linear differential equations have been solved by finite difference method to get the velocity distribution. The flow behavior for Newtonian fluid along a duct channel has been studied with the effect of mass transfer [12]. Here the solution is obtained with different parametric effect such as driving force, blowing parameter and normalized conductance. The stability condition is analyzed for natural convection flow in an inclined duct channel for three dimensional plot [13].On that work it is recognized that the two dimensional flow field is not suitable for natural convection flow in the duct that is placed in parallel. The convection heat exchange of water close to vital region in a duct model has been studied [14]. Here the exchange of thermal energy is much more on the undersurface compared to other two surfaces for the effect of pressure. The flow behavior for inertia effect is investigated through a duct of square cross section [15].Here the effect of Coriolis force and the antithetical effects of stress difference of first and second order is studied. In a duct of square cross section the flow pattern for liquid crystal flow with the effect of magnetic diapole has been studied [16]. On that paper they have presented the flow phenomena for developing flow with periodic boundary conditions through square duct. The effect of strong transverse magnetic field for steady flow of liquid metal through a duct channel has been investigated [17]. Here the result is performed for different values of Hartmann number and Prandtl number and the velocity profile is shown for the MHD effect. The experimental result has been shown for pseudo plastic fluid passing through a duct of square cross section [18]. Here the flow rates are shown for fluctuating pressure on walls and the velocity profile is compared with bench mark experiments for laminar and turbulent flow. The fluid flow of dense swarm of particles with viscous force effect has been shown [19]. Here the flow behavior is described by Darcy's equation through porous medium. The flow of the fluid with effects of heat and mass transfer having compliant walls has been investigated through darcy-Brinkman-Forchheimer porous medium [20]. On that paper the non-linear differential equations have been solved using Homotopy perturbation

technique to get exact wavelength of peristaltic wave and small Reynolds number. The magnetohydrodynamics (MHD) effect on blood flow of Jeffery fluid model through porous medium has been investigated [21]. Here the partial differential equations with long wavelength have been solved for Jeffrey fluid model. Flow behavior in Bronchial tree of human lung with Lumped-Model parameter has been studied [22]. Here the parallel lumped model is solved analytically to explain the dynamic behavior of the fluid. The velocity profile is shown by taking porosity parameter as zero, which represents the velocity profile for clear medium [5].

With the above discussions, we have studied the flow behavior in 11th generation of human lung channel through porous medium. The channel is considered as porous medium with homogeneous pore. The numerical solutions of the governing partial differential equations have been obtained using finite difference method. Flow rates are presented graphically for different fluid parameters. Finally a comparison for pressure gradient between porous and non-porous medium is illustrated.

2. Respiratory Branches and Function of Lungs

The lung is an important organ that takes part in gas exchange process. In pulmonary hyperinflation process, the muscles of thoracic cage extend the lung tissues to increase the volume and then air is breathed into it. In artificial ventilation process air is sucked into the human lung by increased outside pressure. Human lung consists of a structure like branching tree to distribute the breathing air in different parts of consecutive generations of channels. The area of each cross section of ducts is increased in next generation and for that the air flow is dropped off to reach the lowest velocity in last generations. In last generations (G22-G23) of ducts there are the alveoli which are separated by thin membrane consists of blood. The alveoli are convex polyhedron like air bubbles bounded by tissue layer where diffusion occurs. When the thoracic wall is relax, the internal pressure extended the lung tissues to remove air by expanding the chest wall. In human lung there are around 300 million alveoli. The diameter of the alveoli is nearly 0.3 mm. The alveoli fill up almost 90% of the lung volume containing small air ducts whose diameter is 0.3 to 1 mm. In the structure of lung model the most farthest alveolus from respiratory bronchioles contains around 2.5 to 3 litres of air where an adult lung can take around 5 litres of air. Actually the gas exchange takes place in the alveolated region to maintain molecular diffusion. According to respirational function and its anatomical configuration, the lung consists of two regions called air transport and gas diffusion. The airways from tracheal to terminal bronchioles are fractionalized repeatedly and gas is delivered without any gas exchange.

Table 2. 1: Approximate quantification of the human bronchial system (Weibel's model)

	Generation(G)	Number (n)	Mean diameter[mm]	Length [mm]	Volume [ml]	Re
Trachea	0	1	18.00	120.00	30.54	1480
Main Bronchus	1	2	12.20	47.60	11.13	1092
Lobar Bronchus	2	4	8.30	19.00	4.11	803
	3	8	5.60	7.60	1.50	595
Segmental Bronchus	4	16	4.50	12.70	3.23	370
Bronchi w/	5	32	3.50	10.70	3.29	238

Cartilage in Wall	6	64	2.80	9.00	3.55	149
	7	128	2.30	7.60	4.04	91
	8	256	1.96	6.40	4.94	53
	9	512	1.54	5.40	5.15	34
	10	1024	1.30	4.60	6.25	20
Terminal Bronchus	11	2048	1.09	3.90	7.45	12
Bronchiole w/ muscle in wall	12	4096	0.96	3.30	9.78	6.78
	13	8192	0.82	2.70	11.68	3.97
	14	16384	0.74	2.30	16.21	2.20
	15	32768	0.66	2.00	22.42	1.23
Terminal Bronchiole	16	65536	0.60	1.65	30.57	0.68
Respiratory Bronchiole	17	131072	0.54	1.41	42.33	0.38
	18	262144	0.50	1.17	60.22	0.20
	19	524288	0.47	0.99	90.05	0.11
Alveolar Duct	20	1048576	0.45	0.83	138.42	0.056
	21	2097152	0.43	0.70	213.18	0.030
	22	4194304	0.41	0.59	326.72	0.015
Alveolar Sac	23	8388608	0.41	0.50	553.75	0.008
Alveoli. 21 Per duct		3E+0	0.E+2	0.E+3		

According to the measurement of lung tree and its anatomy, the human airway of lung is shown in Fig. 2.1. It is drawn by performing the calculation of Weibel's real data analysis for adult lung.
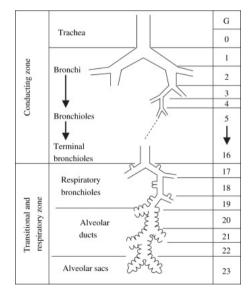

Fig. 2.1. Idealization of the human airways (according to Weibel, 1963).

3.   Formulation and Model Equations of the Problem

We consider the 11thgeneration of human lung channel as a rectangular porous duct with uniform cross section. The steady flow is maintained along this channel. Cartesian coordinate system is taken for the flow measurements. The axis of duct channel is z-axis and x, y-axes are considered as width and height of the duct respectively. Let $x = a$ be the width, $y = a$ be the height and $z = l$ be the length of the rectangular duct. The flow occurs in positive z direction. So the flow rate along z-direction with constant pressure can be considered as
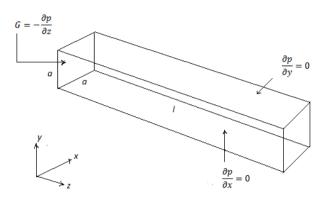
$$q = (0, 0, w(x, y))$$

Fig. 3.1. Geometry of the problem

The equations governing the steady flow along human lung channel of porous medium with porosity effect are the following continuity and linear momentum equation as Brinkman [19].

$$\nabla.q = 0 \tag{3.1}$$

$$-\nabla p + \mu^* \nabla^2 q - \phi R q = 0 \tag{3.2}$$

Where q is the flow rate, ϕ is porosity of the fluid, p is pressure gradient, $\mu^*$is the viscosity of the fluid saturating to the porous medium and R is the Darcy resistance as

$$R = \frac{\mu}{k} q$$

Where μ is base fluid viscosity and k is the permeability parameter.

The flow rate $q = (0,0, w(x, y))$satisfies equations (3.1) and (3.2) and then we have

$$\frac{\partial w}{\partial z} = 0 \tag{3.3}$$

$$\mu^* \left(\frac{\partial^2 w}{\partial x^2} + \frac{\partial^2 w}{\partial y^2} \right) - \frac{\mu\phi}{k} w - \frac{\partial p}{\partial z} = 0 \tag{3.4}$$

Where $\nabla^2 = \dfrac{\partial^2}{\partial x^2} + \dfrac{\partial^2}{\partial y^2}$

The no-slip boundary conditions for the flow are

$$w(x,0) = 0 = w(x,a) \text{ for } 0 \le x \le a$$

$$w(0,y) = 0 = w(a,y) \text{ for } 0 \le y \le a$$

Introducing non-dimensional variables

$$\bar{x} = \frac{x}{a}, \quad \bar{y} = \frac{y}{a}, \quad \bar{z} = \frac{z}{l}, \quad \bar{w} = \frac{\rho a}{\mu} w, \quad \bar{p} = \frac{\rho a^2}{\mu^2} p, \quad \sigma^2 = \frac{a^2}{k}.$$

After simplification and dropping bars, equation (3.4) can be written as

$$\frac{\partial^2 w}{\partial x^2} + \frac{\partial^2 w}{\partial y^2} - \phi \lambda \sigma^2 w + c\lambda G = 0 \tag{3.5}$$

In which $G = -\dfrac{\partial p}{\partial z}$, $c = \dfrac{a^3}{l^3}$ and $\lambda = \dfrac{\mu}{\mu^*}$

The non-dimensional boundary conditions are satisfied as

$$w(x,0) = 0 = w(x,1) \text{ for } 0 \le x \le 1 \tag{3.6}$$

$$w(0,y) = 0 = w(1,y) \text{ for } 0 \le y \le 1 \tag{3.7}$$

4. Numerical Scheme of the Problem

4.1. Porous medium

The momentum equation governing the flow (3.5) is solved numerically along with the boundary conditions (3.6) and (3.7) using central difference scheme of finite difference method. The central difference schemes are as follows:

$$\left(\frac{\partial^2 w}{\partial x^2}\right)_{i,j} \approx \frac{w_{i+1,j} - 2w_{i,j} + w_{i-1,j}}{h^2} \tag{4.1}$$

$$\left(\frac{\partial^2 w}{\partial y^2}\right)_{i,j} \approx \frac{w_{i,j+1} - 2w_{i,j} + w_{i,j-1}}{k^2} \tag{4.2}$$

Using (4.1) and (4.2) in (3.5) and taking $h = k$, we obtain

$$w_{i+1,j} - 2w_{i,j} + w_{i-1,j} + w_{i,j+1} - 2w_{i,j} + w_{i,j-1} - \phi \lambda h^2 \sigma^2 w_{i,j} + h^2 c\lambda G = 0$$

$$or, \; w_{i,j} = \frac{1}{\left(4 + \phi \lambda h^2 \sigma^2\right)} \left\{ w_{i+1,j} + w_{i-1,j} + w_{i,j+1} + w_{i,j-1} \right\} + \frac{h^2 c\lambda G}{\left(4 + \phi \lambda h^2 \sigma^2\right)}$$

$$or, \; w_{i,j} = A\left[w_{i+1,j} + w_{i-1,j} + w_{i,j+1} + w_{i,j-1} \right] + B \tag{4.3}$$

Where,

$$A = \frac{1}{4 + \phi \lambda h^2 \sigma^2}$$

$$B = \frac{h^2 c \lambda G}{4 + \phi \lambda h^2 \sigma^2}$$

The difference equation (4.3) gives the algebraic system of equation in terms of $w_{i,j}$.

4.2. Non-porous medium

For non-porous medium, the third term of equation (3.2) vanishes due to $\phi = 0$. After taking dimensionless and simplification it takes the form as

$$\frac{\partial^2 w}{\partial x^2} + \frac{\partial^2 w}{\partial y^2} + Gc = 0 \tag{4.4}$$

Using central difference scheme of finite difference method, equation (4.4) becomes

$$w_{i,j} = \frac{1}{4}\{w_{i+1,j} + w_{i-1,j} + w_{i,j+1} + w_{i,j-1}\} + \frac{h^2 cG}{4} \tag{4.5}$$

In which $G = -\dfrac{\partial p}{\partial z}$ and $c = \dfrac{a^3}{l^3}$

5. Result and Discussions
5.1. Porous medium

The flow rate for different flow parameters are presented graphically in this section. Fig. 5.1 represents the flow rate for different values of pressure gradient. The physical variables are kept limited to the lung model channel and flow is measured for the values of $\lambda = 0.4, \phi = 0.7, \sigma = 0.01$ and $c = 0.02$.
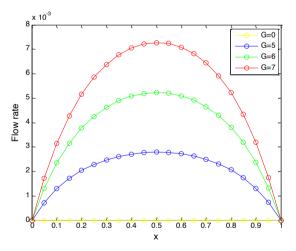

Fig. 5.1. Variations of flow rate for different values of pressure gradient (G) where $\lambda = 0.4, \phi = 0.7, \sigma = 0.01$ and $c = 0.02$

As the pressure gradient is increasing, the flow rate is gradually increasing and developing to parabolic. It can be seen that no flow occurs if the pressure gradient is zero. In Fig. 5.1 it is noted that other parameters are kept fixed . Fig. 5.2 shows the variations of flow rate for different values of Porosity parameter. The porosity indicates how much of fluid can

flow through the pore of lung channel. If the pore quality is good and sufficiently large more amount of fluid will be passed through the porous medium. It can be seen from Fig. 5.2 that when the porosity is increased the flow rate is also increased in the channel. As a result the flow of oxygen will be increased. So it can be said that the flow rate is an increasing function of porosity parameter.
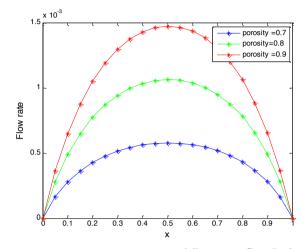

Fig. 5.2. Variations of flow rate for different values of porosity (ϕ) where $G = 5, \lambda = 0.4, \sigma = 0.01$ and $c = 0.02$
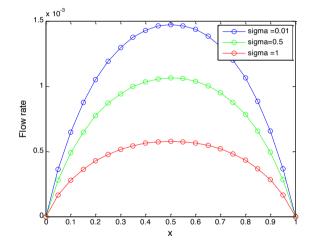

Fig. 5.3. Variations of flow rate for different values of $\sigma \left(= a^2/k \right)$ where $G = 5, \lambda = 0.4, \phi = 0.7$ and $c = 0.02$

Fig. 5.3 represents the flow rate for different values of σ where the dimensionless parameter σ is related with permeability parameter. Permeability parameter represents the flow ability of the fluid per unit area through porous medium. If permeability increases in human lung channel, a little bit more amount of oxygen can flow through porous medium because of permeability property. The decreasing of dimensionless parameter σ, indicates that the permeability constant is higher. So, the flow rate is increasing due to the lower value of σ or higher value of permeability constant k. So it can be said that the flow rate is a decreasing function of dimensionless parameter σ.
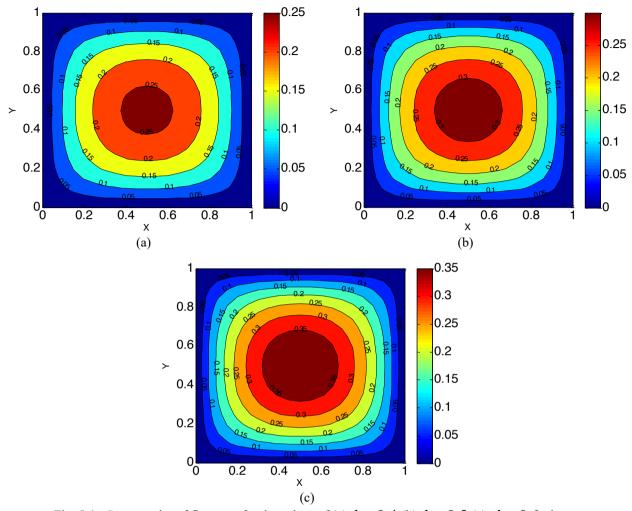
Fig. 5.4. Contour plot of flow rate for the values of (a) $\lambda = 0.4$ (b) $\lambda = 0.5$ (c) $\lambda = 0.6$ where
$$G = 5, \phi = 0.7, \sigma = 0.01 \text{ and } c = 0.02$$

The flow rate for different values of effective viscosity is shown in Fig. 5.4. It is observed that flow rate is higher for higher value of effective viscosity. On the contrary, flow rate becomes higher for the lower value of viscosity of porous medium. Different values of effective viscosity (0.4, 0.5, and 0.6) are taken and the contour in Fig. 5.4 shows the flow phenomena. When the effective viscosity is gradually increased, the flow rate is also gradually increased. It is noticed that the flow rate is increased in Fig. 5.4(b) by 0.3 compared with Fig. 5.4(a) by 0.25 and it is increased in Fig. 5.4(c) by 0.35 compared with Fig. 5.4(b). So it can be said that the flow rate is an increasing function of effective viscosity.

5.2. Non-porous medium

The governing partial differential equations have been solved numerically for non-porous medium also. Fig. 5.5 shows the flow rate for different values of pressure gradient in porous and non-porous medium.
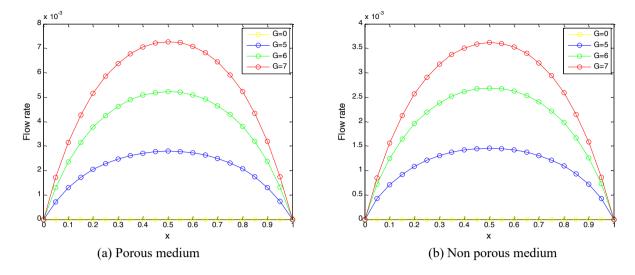
(a) Porous medium   (b) Non porous medium

Fig. 5.5. Variations of flow rate for different values of G where in (a) for porous medium $\lambda = 0.4, \phi = 0.7, \sigma = 0.01$ and $c = 0.02$ (b) for non-porous medium $c = 0.02$.

The same values of pressure gradient in both medium (porous and non-porous) are taken. The highest flow rate is found at $x = 0.5$ for both medium. It is depicted that the flow rate is increased in porous medium compared with non-porous medium. The flow rate of porous medium is almost two times larger than that of non-porous medium. It is observed that no flow takes place for both medium when the pressure gradient is zero.

Conclusion

The flow behavior in 11th generation of human lung channel through porous and non-porous medium has been studied. Duct model of lung channel and Cartesian measurement are considered. The numerical experiment is performed using finite difference central scheme with second order accuracy. The flow characteristics are presented graphically in two dimensional plots. We have found that the flow rate is increased due to the increasing values of pressure gradient (G), porosity (the ratio of pore volume to the total volume) (ϕ), effective viscosity (λ) and dimensionless parameter (σ) which is related with permeability parameter. The flow behavior for non-porous medium is investigated and compared with porous medium in case of pressure gradient. It is noticed that the flow rate is increased in porous medium than that of non-porous medium. The flow rate is almost double in porous medium compared to non-porous one.

Conflict of Interests

The authors declare that there is no conflict of interest regarding the publication of this paper.

Funding

The authors declare that there was no fund available.

References

[1] M. H. Tawhai and C. L. Lin, Imaged-based modeling of lung structure and function, *Journal of Magnetic Resonance Imaging*, 32: 1421–1431 (2010).

[2] R. Watson, Z. Fu, J. B. West, Minimal distensibility of pulmonary capillaries in avian lungs Compared with mamalian lungs, *Respiratory Physiology & Neurobiology* , 160: 208–214 (2008).

[3] Weibel E. R., Morphometry of the human lung, Springer-Verlag, New York, 1963.

[4] W. S. Almalki and M. H. Hamdan, Investigations in Effective Viscosity of Fluid in a Porous Medium, *Int. Journal of Engineering Research and Applications*, 6: 41-51 (2016).

[5] M. Devakar, K. Ramesh, S. Chouhan & A. Raje, Fully developed flow of non-Newtonian fluids in a Straight unifor -m square duct through porous medium, *journal of the Association of Arab Universities for Basic and Applied Sciences*, 23: 66-74 (2017).

[6] N. A. S. Afifi and N. S. Gad, Interaction of peristaltie flow with pulsatile magneto-fluid through a porous medium, *Acta Mechanica*, 149: 229-237 (2001).

[7] A. Zeeshan and R. Ellahi, Series solutions for nonlinear partial differential equations with slip boundary conditions for non-Newtonian MHD fluid in porous space, *Applied Mathematics and Information Sciences*, 7 (1): 257-265 (2013).

[8] B.G. Prasad and A. Kumar, Flow of a hydromagnetic fluid through porous media between permeable beds under exponentially decaying pressure gradient, *Computational Methods in Science and Technology,* 17(1-2): 63-74 (2011).

[9] M. Rahman and S.Y. Ahmad, Finite element analysis of axial flow with heat transfer in a square duct, *Applied Math and Modelling*, 6: 481-490 (1982).

[10] A. E. Cook and M. Rahman, Temperature and velocity distributions in a square duct, *Applied Math and Modelling*, 10: 221-223 (1986).

[11] M. E. Sayed Ahmed, Laminar heat transfer for thermally developing flow of a Herschel-Bulkley fluid in a square Duct, *Int. Comm. Heat Mass Transfer* , 27 (7):1013-1024 (2000).

[12] S. Beale, Mass transfer in plane and square ducts, *International Journal of Heat and Mass Transfer,* 48: 3256–3260 (2005).

[13] T. Adachi, Stability of natural convection in an inclined square duct with perfectly conducting side walls, *International Journal of Heat and Mass Transfer*, 49: 2372–2380 (2006).

[14] S. H. Lee, Convective heat transfer to water near the critical region in a horizontal square duct, *International Journal of Heat and Mass Transfer*, 51: 2930–2939 (2008).

[15 M. Norouzi, M. H. Kayhani, C. Shu, M. R. H. Nobari, Flow of second order fluid in a curved duct with square Cross section, *Journal of Non-Newtonian Fluid Mechanics*, 165: 323–339 (2010).

[16] S. Tympel, D. Krasnov,T. Boeck, J. Schumacher, Distortion of liquid metal flow in a square duct due to the Influence of a magnetic point dipole, *Proc. Appl. Math .Mech*, 12: 567-568 (2012).

[17] D. Sarma, G. C. Hazarika, P. N. Deka, Numerical study of liquid metal mhd flow through a square duct, *International Journal of Computer Applications,* 71(8): 29-32 (2013).

[18] M. A. Kun, Y. Shiwei, C. Huaijian, L. Huanxin, Experimental study of pseudoplastic fluid flows in a Square duct of strong curvature, *Journal of Thermal Science* , 23(4): 359−367 (2014).

[19] H. C. Brinkman, A Calculation of the viscous force exerted by a flowing fluid on a dense swarm of particles, *Applied Scientific Research*, A1: 27-34(1947).

[20] M. M. Bhatti, A. Zeeshan, R. Ellahi, G. C. Shit, Mathematical modeling of heat and mass transfer effects on MHD peristaltic propulsion of two-phase flow through a Darcy-Brinkman-Forchheimer porous medium, *Advanced Powder Technology*, Article in press, Japan (2018).

[21] M. M. Bhatti, M. Ali. Abbas, Simultaneous effects of slip and MHD on peristaltic blood flow of Jeffrey fluid model through a porous medium, *Alexandria Engineering Journal*, Article in press, Egypt (2016).

[22] M. U. Ahmmed and M. Sultana, Study on Flow Behavior of Parallel Lumped-Model under Constant Flow for Bronchial Tree, *GANIT: Journal of Bangladesh Mathematical Society,* 40(2): 86-94 (2020).

Nomenclature	
Symbol	**Meaning**
q	Flow rate, m/s
p	Pressure, Pa
x	x-co-ordinate
y	y-co-ordinate
z	z-co-ordinate
R	Darcy resistance (a measure of the resistance to airflow of a duct), $kgm^{-2}s^{-2.}$
∇	Change in a quantity
μ	Base fluid viscosity, kg/ms
μ^*	Viscosity of the fluid saturating the porous medium, kg/ms
ϕ	Porosity (represents the ratio of pore volume to the total volume)
k	Permeability (indicates the ability of fluids to flow through porous medium), $m^2.$
a	Width and height of duct channel, m
l	Length of duct channel, m
ρ	Density of fluid, kg/m^3
λ	Effective viscosity, $\lambda = \mu/\mu^*$
σ	Dimensionless parameter, $\sigma^2 = a^2/k$
c	Dimensionless parameter, $c = a^3/l^3$